




# New thresholds in semi-quantitative [ $^{18}\text{F}$ ]FDG PET/CT are needed to assess large vessel vasculitis with long-axial field-of-view scanners

Luisa Knappe<sup>1</sup> · Carola Bregenzer<sup>1</sup> · Nasir Gözlügül<sup>1</sup> · Clemens Mingels<sup>1</sup> · Ian Alberts<sup>1</sup> · Axel Rominger<sup>1</sup> · Federico Caobelli<sup>1</sup> 

Received: 9 July 2023 / Accepted: 30 August 2023  
© The Author(s) 2023

## Abstract

**Aim** [ $^{18}\text{F}$ ]FDG PET/CT proved accurate in the diagnostic work-up of large vessel vasculitis (LVV). While a visual interpretation is currently considered adequate, several attempts have been made to integrate it with a semiquantitative evaluation. In this regard, there is the need to validate current or new thresholds for the semiquantitative parameters on long-axial field of view (LAFOV) scanners.

**Methods** We retrospectively evaluated 100 patients (50 with LVV and 50 controls) who underwent [ $^{18}\text{F}$ ]FDG LAFOV PET/CT. Semiquantitative parameters (SUV<sub>max</sub> and SUV<sub>mean</sub>) were calculated for large vessels in 3 districts (supra-aortic [SA], thoracic aorta [TA], and infra-aortic [IA]). Values were also normalized to liver activity (SUV<sub>max</sub>/L-SUV<sub>max</sub>, and SUV<sub>max</sub>/L-SUV<sub>mean</sub>).

**Results** Of the 50 patients diagnosed with LVV, SA vessels were affected in 38 (76%), TA in 42 (84%) and IA vessels in 26 (52%). To-liver normalized values had higher diagnostic accuracy than non-normalized values (AUC always  $\geq 0.90$  vs. 0.74–0.89). For the SA vessels, best thresholds were 0.66 for SUV<sub>max</sub>/L-SUV<sub>max</sub> and 0.88 for SUV<sub>max</sub>/L-SUV<sub>mean</sub>; for the TA, 1.0 for SUV<sub>max</sub>/L-SUV<sub>max</sub> and 1.30 for SUV<sub>max</sub>/L-SUV<sub>mean</sub>; finally, for IA vessels, the best threshold was 0.83 for SUV<sub>max</sub>/L-SUV<sub>max</sub> and 1.11 for SUV<sub>max</sub>/L-SUV<sub>mean</sub>.

**Conclusion** LAFOV [ $^{18}\text{F}$ ]FDG-PET/CT is accurate in the diagnostic workup of LVV, but different threshold in semi-quantitative parameters than reported in literature for standard scanners should be considered.

**Keywords** Large vessel vasculitis · [ $^{18}\text{F}$ ]FDG PET · Long-axial field-of-view PET · Total-body PET · Inflammation

## Introduction

$^{18}\text{F}$ -2-Fluoro-2-deoxy-D-glucose ([ $^{18}\text{F}$ ]FDG) positron emission tomography/computed tomography (PET/CT) has secured an important role in the diagnosis and follow-up of large vessel vasculitis (LVV) [1–3]. Current guidelines recommend a visual evaluation of [ $^{18}\text{F}$ ]FDG PET with a standardized grading system based on the comparison with liver uptake, wherein uptake in a vessel equal to that of the liver is rated as possibly positive (grade 2) and uptake greater than that in the liver as definitively positive (grade 3) [4].

Although visual interpretation is robust if readers are expert, semi-quantitative values have been suggested, which may help in the diagnostic work-up by increasing readers' confidence. In two recent publications, the ratio between maximum standardized uptake value (SUV<sub>max</sub>) within a large vessel and the mean SUV in the liver (L-SUV<sub>mean</sub>) has been suggested as the most accurate semi-quantitative parameter for the diagnosis of LVV. Specifically, a ratio of 1.0 for supra-aortic (SA) vessels and 1.3 for thoracic aorta (TA) and infra-aortic (IA) vessels yielded the best diagnostic performance [5, 6].

However, validated semi-quantitative values and their thresholds rely on studies featuring analogue PET scanners only. It is well known that semi-quantitative parameters, especially SUV<sub>max</sub> can vary considerably across different scanners [7, 8]. This appears of utmost importance for studies performed on newer generation digital scanners,

✉ Federico Caobelli  
federico.caobelli@insel.ch

<sup>1</sup> Department of Nuclear Medicine, Inselspital, University Hospital Bern, University of Bern, Freiburgstrasse 18, 3011 Bern, Switzerland

including long-axial field-of-view (LAFOV) PET/CT systems. The limited resolution and poor signal recovery of small structures such as the vessel wall are partially overcome by digital systems using silicon photomultiplier (SiPM) systems [9]. Such scanners have improved spatial and temporal resolution compared to analogue systems [8, 10] and impact thresholds in the semiquantitative evaluation in the assessment of LVV.

As such, we aimed to evaluate the diagnostic accuracy of various semi-quantitative parameters in [ $^{18}\text{F}$ ] FDG LAFOV PET/CT and to identify the most accurate thresholds.

## Materials and methods

### Patient population

We retrospectively evaluated the first 50 patients with a final clinical diagnosis of LVV who had undergone [ $^{18}\text{F}$ ] FDG PET/CT for the diagnostic work-up of LVV starting from November 2020. All patients were referred for evaluation of a new diagnosis of LVV. No patients were included who underwent therapy assessment or follow up in known LVV. The final diagnosis of LVV was reached in a multidisciplinary setting based on laboratory results, clinical symptoms and imaging results (ultrasound and PET). All patients were scanned on a LAFOV PET/CT system (Biograph Vision Quadra, Siemens Healthineers, Erlangen, Germany) within 48 h from the first clinical consult, wherein LVV was suspected. As control group, another 50 patients were randomly selected from our oncologic database. To that end, all patients were free from signs of vasculitis. Patients with lymphomas, those referred for the search for infectious or inflammatory foci and those patients under therapy with monoclonal antibodies were excluded.

### Imaging protocol

Patients fasted for at least 6 h prior to scanning, blood glucose levels were always  $< 120$  mg/dl (6.7 mmol/L). Sixty minutes after the intravenous administration of a weight-adapted activity of [ $^{18}\text{F}$ ]FDG (3.0 MBq/kg), images were acquired on the LAFOV PET/CT scanner in list-mode for 10 min in a single bed position (skull-vertex to mid femur). Image reconstruction was performed as previously described using high sensitivity mode (HS, maximum ring difference of 85) [10].

Whole body PET images were reconstructed in 3D to a  $440 \times 440 \times 644$  matrix with a voxel size of  $1.65 \times 1.65 \times 1.65$  mm<sup>3</sup>, with a zoom factor of 1.0 using the proprietary time of flight (TOF) point-spread-function (PSF) algorithm with 4

iterations and 5 subsets. A Gauss filter was applied (2-mm FWHM). Emission data were corrected for randoms, scatter, and decay. Non-contrast enhanced, low-dose CT images were used for attenuation correction, parameters have been also previously published [8].

### Image evaluation

Images were visually and semi-quantitatively evaluated using appropriate workstation (Syngo.via MMONcology, Siemens Healthineers, Erlangen, Germany). Semi-quantitative parameters ( $\text{SUV}_{\text{max}}$ ,  $\text{SUV}_{\text{mean}}$ , and  $\text{SUV}_{\text{peak}}$ , respectively) were calculated in the relevant large vessels by manually placing a volume-of-interest (VOI) with a 40%-iso-contour around their whole diameter. Large vessels were divided into three groups: (1) SA vessels: temporal, carotid and subclavian arteries; (2) TA; and (3) IA vessels: abdominal aorta, external/internal iliac, and femoral arteries. Values were calculated for each group, as mean of the single values of all the relevant large vessels.

Consistent with previous reports [5], to-liver normalized values were also calculated for all vessels as the ratio of  $\text{SUV}_{\text{max}}$  of the relevant vessel to  $\text{SUV}_{\text{max}}$  of the liver ( $\text{L-SUV}_{\text{max}}$ ) and  $\text{SUV}_{\text{mean}}$  of the liver ( $\text{L-SUV}_{\text{mean}}$ ). To that end, these semi-quantitative parameters were calculated for the liver also by placing a standard 10 cm<sup>3</sup> VOI in healthy liver tissue in the right lobe. To-blood pool (BP) normalized values were also calculated, by placing a standard  $2 \times 2$  pixels wide VOI centred at the mitral valve plane.

### Statistical analysis

Statistical analysis was carried out using IBM SPSS (Version 28.0.1.1, IBM Corp. Armonk, NY, USA). Data are presented as mean  $\pm$  SD. Comparison between continuous variables in patients with and without LVV was tested using Mann–Whitney *U* test. The diagnostic accuracy of different semi-quantitative parameters was evaluated by means of receiver-operating-characteristic (ROC) curves analysis on a per-patient basis (with 95% CI) with calculation of Youden Index for the assessment of the best thresholds. *P* values  $< 0.05$  were considered statistically significant.

## Results

### Semi-quantitative parameters

Of the 50 patients diagnosed with LVV, SA vessels were affected in 38 (76%), thoracic aorta in 42 (84%), and IA

**Table 1** Clinical characteristics of the patients with LVV

Clinical characteristic	n (%)
Amaurosis fugax	3 (6.0%)
Loss of vision	2 (4.0%)
New onset headache	24 (48.0%)
Jaw claudication	1 (2.0%)
Scalp tenderness	10 (20.0%)
Pathological temporal artery	7 (14.0%)
Proximal muscle pain	19 (38.0%)
Fever	8 (16.0%)
Erythrocyte sedimentation rate	62 mm/h (16–101)
C-reactive-protein	24.3 mg/L (10–61)

vessels in 26 (52%). Clinical characteristics are displayed in Table 1. Only 3 patients with LVV (6.0%) presented with the involvement of only one segment (2 with involved temporal arteries and 1 with left subclavian artery), while the majority of patients had multilevel involvement. All semi-quantitative parameters were significantly different between patients with and without LVV (Table 2). Of note, L-SUV<sub>max</sub> was also different between patients with and without LVV (2.98 ± 0.13 vs. 3.32 ± 0.14, *p* = 0.027), while L-SUV<sub>mean</sub> was not (2.51 ± 0.10 vs. 2.32 ± 0.09, *p* = 0.125).

**Per-patient diagnostic accuracy**

ROC-curves analysis showed higher diagnostic accuracy for to-liver normalized values (AUC always ≥ 0.90) than for non-normalized ones (AUC 0.74–0.89, Table 2). Best separators were calculated for to-liver normalized values, whose ROC curves are displayed in Figs. 1 and 2. For the SA vessels, best thresholds were 0.66 for SUV<sub>max</sub>/L-SUV<sub>max</sub> and 0.88 for SUV<sub>max</sub>/L-SUV<sub>mean</sub>; for the TA, 1.0 for SUV<sub>max</sub>/L-SUV<sub>max</sub> and 1.30 for SUV<sub>max</sub>/L-SUV<sub>mean</sub>; finally, for IA vessels, the best threshold was 0.83 for SUV<sub>max</sub>/L-SUV<sub>max</sub> and 1.11 for SUV<sub>max</sub>/L-SUV<sub>mean</sub>. The thresholds and their sensitivity and specificity are reported in Table 3. To-blood pool normalized ratio proved less accurate (Supplemental Table).

**Accuracy of to-date suggested thresholds on LAFOV PET**

The currently suggested thresholds showed inferior sensitivity and slight higher specificity when applied to LAFOV PET imaging. Using the current threshold of SUV<sub>max</sub>/L-SUV<sub>mean</sub> = 1.0 for SA vessels, sensitivity was 68% and specificity 90%, (with threshold 0.88 sensitivity was 86% and specificity 80%). Using the threshold of SUV<sub>max</sub>/L-SUV<sub>mean</sub> = 1.3 for IA vessels resulted in sensitivity 80% and specificity 96% for IA vessels (with threshold 1.11, sensitivity 96% and specificity 90%).

**Table 2** Age and semi-quantitative values in patients with and without large vessel vasculitis (LVV). Data are provided as mean ± SD. Area under the curve (AUC) is provided with 95% confidence intervals (CI)

	SA vessels vasculitis			TA vasculitis			IA vessels vasculitis					
	Pos (n=38)	Neg (n=62)	<i>p</i>	AUC (95% CI)	Pos (n=42)	Neg (n=58)	<i>p</i>	AUC (95% CI)	Pos (n=26)	Neg (n=74)	<i>p</i>	AUC (95% CI)
	Age (years)	69.3 ± 9.34 13 (34.2)	66.5 ± 11.7 28 (45.2)	0.283 0.301	- -	68.5 ± 9.97 13 (31.0)	66.9 ± 11.5 28 (48.3)	0.546 0.101	- -	69.2 ± 8.18 8 (30.8)	67.0 ± 11.7 33 (44.6)	0.563 0.253
Male gender, n (%)	3.48 ± 1.53	1.89 ± 0.57	<0.01	0.81 (0.73–0.90)	4.62 ± 1.69	2.50 ± 0.97	<0.01	0.88 (0.81–0.95)	4.02 ± 1.41	2.95 ± 1.47	<0.01	0.89 (0.83–0.96)
SUV <sub>max</sub>	1.92 ± 0.67	1.28 ± 0.39	<0.01	0.76 (0.67–0.86)	2.12 ± 0.61	1.60 ± 0.62	<0.01	0.78 (0.69–0.87)	2.04 ± 0.62	1.73 ± 0.66	0.012	0.79 (0.70–0.88)
SUV <sub>mean</sub>	2.32 ± 0.87	1.57 ± 0.45	<0.01	0.74 (0.64–0.84)	3.19 ± 0.96	2.06 ± 0.73	<0.01	0.85 (0.77–0.93)	2.69 ± 0.82	2.26 ± 0.92	0.008	0.84 (0.77–0.92)
SUV <sub>max</sub> /L-SUV <sub>max</sub>	1.22 ± 0.61	0.60 ± 0.13	<0.01	0.91 (0.85–0.97)	1.62 ± 0.61	0.77 ± 0.19	<0.01	0.95 (0.92–0.99)	1.45 ± 0.56	0.94 ± 0.45	<0.01	0.98 (0.96–1.00)
SUV <sub>max</sub> /L-SUV <sub>mean</sub>	1.61 ± 0.72	0.80 ± 0.19	<0.01	0.90 (0.84–0.96)	2.07 ± 0.75	1.01 ± 0.26	<0.01	0.94 (0.90–0.99)	1.88 ± 0.68	1.23 ± 0.56	<0.01	0.98 (0.95–1.00)

SUV Standardized uptake value, L-SUV to-liver normalized standardized uptake value, SA supra-aortic vessels, TA thoracic aorta, IA infra-aortic vessels, Pos. patients with LVV, Neg. patients without LVV

**Fig. 1** ROC-curves analysis for normalized maximum standardized uptake value ( $SUV_{max}$ ) of the relevant vessels to liver  $SUV_{max}$  ( $L-SUV_{max}$ ). SA = supra-aortic vessels; TA = thoracic aorta; IA = infra-aortic vessels

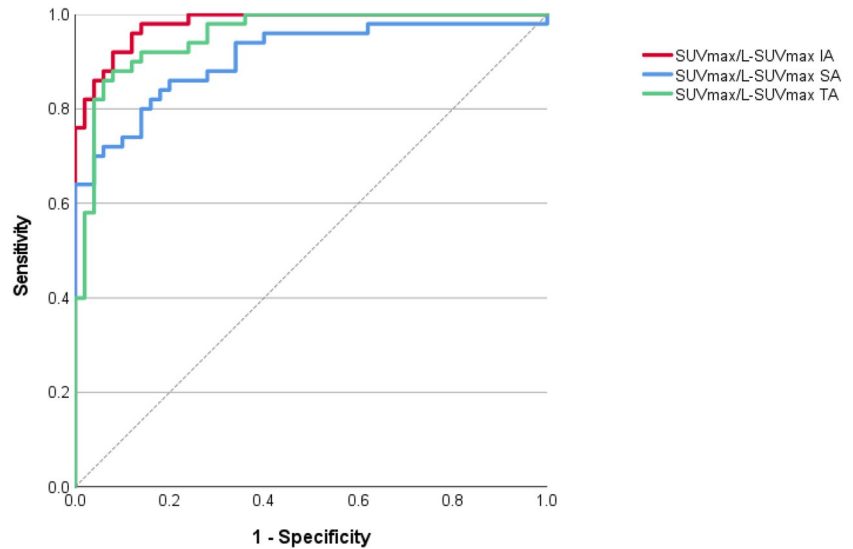


**Fig. 2** ROC-curves analysis for normalized maximum standardized uptake value ( $SUV_{max}$ ) of the relevant vessels to liver  $SUV_{mean}$  ( $L-SUV_{mean}$ ). SA = supra-aortic vessels; TA = thoracic aorta; IA = infra-aortic vessels

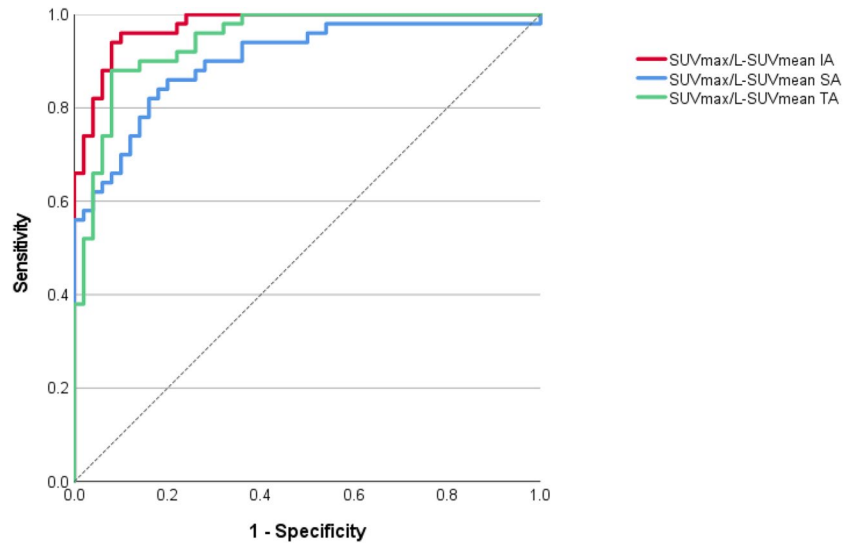


**Table 3** Best separators for semi-quantitative values with values of sensitivity and specificity

	Threshold	Sensitivity	Specificity
$SUV_{max}$ SA/ $L-SUV_{max}$	0.66	86%	80%
$SUV_{max}$ AT/ $L-SUV_{max}$	1.00	88%	92%
$SUV_{max}$ IA/ $L-SUV_{max}$	0.83	98%	86%
$SUV_{max}$ SA/ $L-SUV_{mean}$	0.88	86%	80%
$SUV_{max}$ AT/ $L-SUV_{mean}$	1.30	88%	92%
$SUV_{max}$ IA/ $L-SUV_{mean}$	1.11	96%	90%

$SUV$  Standardized uptake value,  $L-SUV$  to-liver normalized standardized uptake value, SA supra-aortic vessels, TA thoracic aorta, IA infra-aortic vessels

## Discussion

While current guidelines recommend visual interpretation only in PET imaging in the assessment of LVV, recent evidence suggests that semi-quantitative methods may be preferred in clinical practice. Besides the abovementioned report on semi-quantitative parameters able to assist the clinicians in the diagnosis of LVV [5, 6], other scoring systems have been recently suggested [11], also able to differentiate between LVV and atherosclerosis with very good accuracy.

In this regard, it should be noted that a meta-analysis showed that the pooled sensitivity of a visual interpretation

is good but not excellent, ranging between 75.9 and 83.3% using the clinical diagnosis as reference standard [12]. Adding also uptake intensity to the visual analysis yields higher diagnostic accuracy, as demonstrated by a recent prospective study featuring 64 patients with suspected giant cell arteritis, wherein PET had sensitivity 92% and specificity 85% [13].

As such, there is a clear rationale to pursue a semi-quantitative evaluation in PET imaging interpretation, although to-date there is still insufficient evidence of a superiority over visual interpretation only [3, 14]. However, another two questions arise: (1) what is the best semi-quantitative parameter and with which separator? and (2) is there a chance that semi-quantitative thresholds are not interchangeable across different PET scanners?

Our work expands on this topic, confirming that the to-liver normalized semi-quantitative values yield higher accuracy than non-normalized ones, consistent with previous reports [5, 6]. But in contrast to the previous works, we here demonstrate a substantial equivalence between  $SUV_{max}/L-SUV_{max}$  and  $SUV_{max}/L-SUV_{mean}$  in all vascular territories. Furthermore, we provide for the first time data on the diagnostic accuracy of semi-quantitative PET using LAFOV scanners.

We found that the best separators are lower than reported for conventional, analogue PET systems. The most conceivable explanation relies on the intrinsic differences in the scanners. On LAFOV PET, using a 10-min acquisition 1 h post injection reduces the background noise compared to a standard-axial field-of-view scanner (SAFOV) [15]. Moreover, using the advantage of covering all coincidences in the whole FOV simultaneously with a LAFOV system leads to a gain in scanner sensitivity. It should be noted that the exact contribution from digital vs. analogue systems rather than LAFOV vs. SAFOV could not be elucidated.

Thresholds reported in the literature should be decreased and updated when scanning patients on LAFOV PET systems, in order to avoid false negative findings. It should be acknowledged that the to-date established  $SUV_{max}/L-SUV_{mean}$  threshold of 1.3 is adequate for inflammation involving the thoracic aorta. We highly recommend using normalized values as we showed to avoid inter-individual variations of [ $^{18}F$ ]FDG-uptake.

Taken together, our results seem to indicate a complementary role of the semi-quantitative PET analysis. As a matter of fact, a global scan assessment by PET-experienced nuclear medicine physicians including both visual and semi-quantitative analysis provides high accuracy [13], and this may reflect the fact that an experienced reader can weigh the impact of the degree of [ $^{18}F$ ]FDG uptake depending on the location, the pattern of [ $^{18}F$ ]FDG-uptake (i.e., diffuse vs. focal) and the presence of possible atheroma [13].

Some limitations of our study should be acknowledged. First, due to the retrospective nature of the present study, patients already diagnosed with LVV were evaluated, and their results were compared with patients without any clinical and radiologic sign of LVV. Hence, conclusions about our proposed thresholds in patients with clinical signs of LVV but unclear diagnosis may not be fully applicable in clinical practice. To note, the same limitation also pertains to previous studies featuring analogue PET scanners [5, 6]. Furthermore, the patients' sample is relatively small and further prospective studies are needed for their precise definition. However, the main aim of our study was to underline the need for different thresholds when using LAFOV PET, which bears importance in clinical practice for the nuclear medicine community.

It should also be noted that we cannot rule out incorrect information on ongoing steroid therapy in our population. This may have impacted our results, as glucocorticoids may lower [ $^{18}F$ ]FDG uptake and mask a subtending inflammation. In this regard, a recent study showed a decrease in the [ $^{18}F$ ]FDG uptake after 3 days of high-dose glucocorticoids, but without loss of diagnostic accuracy, which only occurred after 10 days of treatment [16]. In clinical practice, the start of glucocorticoid therapy cannot often be delayed during severe clinical symptoms, and therefore, it is conceivable that some of our patients were on steroid therapy at the time of PET/CT. But given the fact that PET was always performed within 48 h from the first clinical visit, it is extremely unlikely that patients were on medications for more than 3 days. Hence, the impact on our values is expected to be negligible.

The multidisciplinary team was aware of the PET/CT results as they provided relevant information for patient management, and this may have an impact on the diagnosis. However, the team has ample clinical experience, and based its judgment on the extensive information available from all sources at the end of the diagnostic work-up. Although this gold standard may be subject to criticism, still it represents a common clinical situation, wherein biopsy cannot be performed, and is adhering to current recommendations [17]. Finally, we could not assess the impact of a different timing of imaging after [ $^{18}F$ ]FDG injection. While different timing was reported to affect the sensitivity for active vasculitis, being higher for later acquisitions [18], our study features the same uptake period post injection of the previous reports, wherein the current thresholds for semi-quantitative PET were suggested. As such, there is a full comparability among our studies, which gives more reliability when assessing the need of different thresholds using LAFOV-PET.

## Conclusion

Our results confirm the importance of [<sup>18</sup>F]FDG-PET/CT in the diagnostic workup of LVV. In this regard, LAVOF PET/CT may yield increased diagnostic accuracy owing to reduced background noise and improved spatial/temporal resolution, but different thresholds in semi-quantitative parameters should be considered. Prospective studies are warranted to implement new reference values in clinical practice when using high sensitivity scanners.

**Supplementary Information** The online version contains supplementary material available at <https://doi.org/10.1007/s00259-023-06423-w>.

**Funding** Open access funding provided by University of Bern

**Data Availability** Data will be made available upon reasonable request.

## Declarations

**Ethical approval** The cantonal ethics committee approved this patient acquisition (KEK-Nr. 2022–00486). All patients provided written informed consent for inclusion. The study was performed in accordance with the Declaration of Helsinki.

**Conflict of interest** Federico Caobelli is currently supported by a research grant by Siemens Healthineers and receives speakers Honoraria by Bracco AG and Pfizer AG for matters not related to the present manuscript. Axel Rominger has received research support and speaker honoraria from Siemens.

**Open Access** This article is licensed under a Creative Commons Attribution 4.0 International License, which permits use, sharing, adaptation, distribution and reproduction in any medium or format, as long as you give appropriate credit to the original author(s) and the source, provide a link to the Creative Commons licence, and indicate if changes were made. The images or other third party material in this article are included in the article's Creative Commons licence, unless indicated otherwise in a credit line to the material. If material is not included in the article's Creative Commons licence and your intended use is not permitted by statutory regulation or exceeds the permitted use, you will need to obtain permission directly from the copyright holder. To view a copy of this licence, visit <http://creativecommons.org/licenses/by/4.0/>.

## References

1. Knappe LM, Verburg FA, Giovannella L, Luster M, Librizzi D. Diagnostic value of FDG-PET/CT in the diagnostic workup of inflammation of unknown origin. *Nuklearmedizin*. 2023;62:27–33.
2. Palestro CJ, Brandon DC, Dibble EH, Keidar Z, Kwak JJ. FDG PET in evaluation of patients with fever of unknown origin: AJR expert panel narrative review. *AJR Am J Roentgenol*. 2023;21:1–12.
3. Slart RHJA, Nienhuis PH, Glaudemans AWJM, Brouwer E, Gheysens O, van der Geest KSM. Role of 18F-FDG PET/CT in large vessel vasculitis and polymyalgia rheumatica. *J Nucl Med*. 2023;64:515–21.
4. Slart RHJA; Writing group; Reviewer group; Members of EANM Cardiovascular; Members of EANM Infection & Inflammation; Members of Committees, SNMMI Cardiovascular; Members of Council, PET Interest Group; Members of ASNC; EANM Committee Coordinator. FDG-PET/CT(A) imaging in large vessel vasculitis and polymyalgia rheumatica: joint procedural recommendation of the EANM, SNMMI, and the PET Interest Group (PIG), and endorsed by the ASNC. *Eur J Nucl Med Mol Imaging*. 2018;45:1250–1269.
5. Imfeld S, Rottenburger C, Schegk E, Aschwanden M, Juengling F, Staub D, Recher M, Kyburz D, Berger CT, Daikeler T. [18F] FDG positron emission tomography in patients presenting with suspicion of giant cell arteritis—lessons from a vasculitis clinic. *Eur Heart J Cardiovasc Imaging*. 2018;19:933–40.
6. Imfeld S, Scherrer D, Mensch N, Aschwanden M, Staub D, Berger CT, Daikeler T, Rottenburger C. A simplified PET/CT measurement routine with excellent diagnostic accuracy for the diagnosis of giant cell arteritis. *Diagnostics (Basel)*. 2022;12:728.
7. Dondi F, Pasinetti N, Gatta R, Albano D, Giubbini R, Bertagna F. Comparison between two different scanners for the evaluation of the role of 18F-FDG PET/CT semiquantitative parameters and radiomics features in the prediction of final diagnosis of thyroid incidentalomas. *J Clin Med*. 2022;11:615.
8. Mingels C, Weidner S, Sari H, Buesser D, Zeimpekis K, Shi K, Alberts I, Rominger A. Impact of the new ultra-high sensitivity mode in a long axial field-of-view PET/CT. *Ann Nucl Med*. 2023;37:310–5.
9. Alberts I, Prenosil G, Sachpekidis C, Weitzel T, Shi K, Rominger A, Afshar-Oromieh A. Digital versus analogue PET in [<sup>68</sup>Ga]Ga-PSMA-11 PET/CT for recurrent prostate cancer: a matched-pair comparison. *Eur J Nucl Med Mol Imaging*. 2020;47:614–23.
10. Alberts I, Sari H, Mingels C, Afshar-Oromieh A, Pyka T, Shi K, Rominger A. Long-axial field-of-view PET/CT: perspectives and review of a revolutionary development in nuclear medicine based on clinical experience in over 7000 patients. *Cancer Imaging*. 2023;23:28.
11. Bacour YAA, van Kanten MP, Smit F, Comans EFI, Akarriou M, de Vet HCW, Voskuyl AE, van der Laken CJ, Smulders YM. Development of a simple standardized scoring system for assessing large vessel vasculitis by 18F-FDG PET-CT and differentiation from atherosclerosis. *Eur J Nucl Med Mol Imaging*. 2023;50:2647–55.
12. Lee YH, Choi SJ, Ji JD, Song GG. Diagnostic accuracy of 18F-FDG PET or PET/CT for large vessel vasculitis : a meta-analysis. *Z Rheumatol*. 2016;75:924–31.
13. Sammel AM, Hsiao E, Schembri G, Nguyen K, Brewer J, Schriber L, Janssen B, Youssef P, Fraser CL, Bailey E, Bailey DL, Roach P, Laurent R. Diagnostic accuracy of positron emission tomography/computed tomography of the head, neck, and chest for giant cell arteritis: a prospective, double-blind, cross-sectional study. *Arthritis Rheumatol*. 2019;71:1319–28.
14. Gheysens O, Jamar F, Glaudemans AWJM, Yildiz H, van der Geest KSM. Semi-quantitative and quantitative [18F]FDG-PET/CT indices for diagnosing large vessel vasculitis: a critical review. *Diagnostics (Basel)*. 2021;11:2355.
15. Alberts I, Hünermund JN, Prenosil G, Mingels C, Bohn KP, Viscione M, Sari H, Vollnberg B, Shi K, Afshar-Oromieh A, Rominger A. Clinical performance of long axial field of view PET/CT: a head-to-head intra-individual comparison of the Biograph Vision Quadra with the Biograph Vision PET/CT. *Eur J Nucl Med Mol Imaging*. 2021;48(8):2395–404.
16. Nielsen BD, Gormsen LC, Hansen IT, Keller KK, Therkildsen P, Hauge EM. Three days of high-dose glucocorticoid treatment attenuates large-vessel 18F-FDG uptake in large-vessel giant cell arteritis but with a limited impact on diagnostic accuracy. *Eur J Nucl Med Mol Imaging*. 2018;45:1119–28.

17. Hellmich B, Sanchez-Alamo B, Schirmer JH, Berti A, Blockmans D, Cid MC, Holle JU, Hollinger N, Karadag O, Kronbichler A, Little MA, Luqmani RA, Mahr A, Merkel PA, Mohammad AJ, Monti S, Mukhtyar CB, Musial J, Price-Kuehne F, Segelmark M, Teng YKO, Terrier B, Tomasson G, Vaglio A, Vassilopoulos D, Verhoeven P, Jayne D. EULAR recommendations for the management of ANCA-associated vasculitis: 2022 update. *Ann Rheum Dis.* 2023:ard-2022–223764.
18. Quinn KA, Rosenblum JS, Rimland CA, Gribbons KB, Ahlman MA, Grayson PC. Imaging acquisition technique influences interpretation of positron emission tomography vascular activity in large-vessel vasculitis. *Semin Arthritis Rheum.* 2020;50:71–6.

**Publisher's Note** Springer Nature remains neutral with regard to jurisdictional claims in published maps and institutional affiliations.